DIAGNOSTYKA, 2016, Vol. 17, No. 2

ISSN 1641-6414
e-ISSN 2449-5220

APPLICATION OF TIME-FREQUENCY DISTRIBUTIONS IN DIAGNOSTIC SIGNAL PROCESSING PROBLEMS: A CASE STUDY

Andrzej KATUNIN

Institute of Fundamentals of Machinery Design, Silesian University of Technology, Konarskiego 18A, 44-100 Gliwice, Poland, e-mail: andrzej.katunin@polsl.pl

Summary

In this paper, the author analyzed an applicability of selected types of time-frequency distributions that belong to Cohen's class and their reassignments for signals similar to those obtained during machinery diagnostics. At the first step of performed studies a synthetic multicomponent signal that contains both stationary and non-stationary components was analyzed using algorithms based on various time-frequency distributions. This allows for evaluating effectiveness of identification of particular components by applied time-frequency distributions and selecting a group of the most effective algorithms. At the second step, the selected time-frequency distributions were applied for analysis of signals acquired during diagnosis of rolling bearings in order to verify the effectiveness of identification of components responsible for a priori known faults occurred in bearings.

Keywords: time-frequency distributions, signal processing, multicomponent identification, bearing fault diagnosis

ZASTOSOWANIE DYSTRYBUCJI CZASOWO-CZĘSTOTLIWOŚCIOWYCH W DIAGNOSTYCZNYM PRZETWARZANIU SYGNAŁÓW: STUDIUM PRZYPADKU

Streszczenie

W niniejszym artykule autor analizuje stosowalność wybranych typów dystrybucji czasowo-częstotliwościowych, które należą do klasy Cohena i ich wersji redefiniowanych dla sygnałów zbliżonych do takich, które są otrzymywane podczas diagnostyki maszyn. W pierwszym kroku przeprowadzonych badań syntetyczny wieloskładowy sygnał, zawierający zarówno stacjonarne jak i niestacjonarne składowe, był analizowany z wykorzystaniem algorytmów opartych na różnych dystrybucjach czasowo-częstotliwościowych. Pozwoliło to na ocenę efektywności identyfikacji poszczególnych składowych przez zastosowane dystrybucje czasowo-częstotliwościowe oraz wybór grupy najefektywniejszych algorytmów. W drugim kroku wybrane dystrybucje czasowo-częstotliwościowe zostały zastosowane do analizy sygnałów pozyskanych podczas diagnostyki łożysk tocznych w celu weryfikacji efektywności identyfikacji składowych odpowiedzialnych za wystąpienie uszkodzeń w łożyskach, znanych a priori.

Słowa kluczowe: dystrybucja czasowo-częstotliwościowa, przetwarzanie sygnałów, identyfikacja wieloskładowa, diagnostyka łożysk tocznych

1. INTRODUCTION

Machinery being operated usually reveals vibrations which is a relevant and often used source of diagnostic information. However, the most of machines generates highly non-stationary multicomponent signals due to presence of components whose statistical features change in time as well as presence of transient components and noise. Several methods used in diagnostics of rotor machinery are focused on acquisition of such non-stationary signals (usually acquired during run-up or run-down of a machine) [1-3] which is a rich source of diagnostic information. Due to the variability of time and frequency features simultaneously in such signals the classical methods of signal analysis in time and frequency domains separately are inappropriate since they assume stationarity in whole analyzed band of a given domain. Thus, the development of methods of joint time-frequency (TF) analysis began extremely important for signal processing issues addressed to machinery diagnostics.

Many efficient methods of TF analysis have been developed to-date. The earliest approach of linear TF representation is the Short-Time Fourier Transform (STFT):

$$\mathrm{STFT}_x(t,f)=\int_{-\infty}^{+\infty}x(\tau)w(\tau-t)\exp(-j2\pi f\tau)\mathrm{d}\tau\,, \quad (1)$$

where $x(t)$ is a signal, $w(\tau–t)$ is a window function centered at time t with a window length of τ, j is an imaginary unit and f is a frequency; which assumes local stationarity in a fixed-size window translated over the signal domain. This means that STFT has a fixed resolution, where the time and frequency resolution depend on each other, i.e. when the time

resolution is high the frequency resolution is low, and vice-versa. This property is related to the Heisenberg uncertainty principle. Further approach of linear TF representation is the Continuous Wavelet Transform (CWT):

$$\mathrm{CWT}_x(t,a)=\frac{1}{\sqrt{a}}\int_{-\infty}^{+\infty}x(\tau)\psi\left(\frac{\tau-t}{a}\right)\mathrm{d}\tau, \quad (2)$$

where the term $\psi([\tau–t]/a)$ is a kernel function obtained from dilating and translating of a wavelet basis $\psi(t)$ and a is the normalization factor used for maintaining energy conservation (usually $a = 2$ [4]). Compared to STFT, CWT has much better resolution properties and ability of localization of singularities in analyzed signal due to a possibility of application of various (almost arbitrary) basis functions, and dilation and scaling properties [5].

Another group of TF representations, developed in parallel to the above-mentioned linear TF representations, is a group of bilinear and higher-order TF representations which belong to Cohen's class of TF distributions (TFDs). The fundamental distribution for the mentioned class (on which it is based) is the Wigner-Ville distribution (WVD):

$$\mathrm{WVD}_x(t,f)=\int_{-\infty}^{+\infty}x\left(t+\frac{\tau}{2}\right)x^*\left(t-\frac{\tau}{2}\right)\cdot\exp(-j2\pi f\tau)\mathrm{d}\tau, \quad (3)$$

where x^* is a complex conjugate of a signal x. This TFD is based on determination of autocorrelation function for further determination of a power spectrum of a signal, similarly as other TFDs belonged to the Cohen's class. WVD is a non-linear (quadratic) distribution, which means that a sum of multiple signal components is not equal to a sum of their WVDs [3]. Since WVD satisfies the most of the mathematical properties and features of optimal TF localization (see [6] for instance), this distribution is optimal in theoretical sense. Due to this fact, WVD is commonly applied in a wide range of practical signal processing problems, like identification of components in transient signals [7], rotating machinery fault detection [8-10], detection of part loose in reactor coolant systems [11], texture segmentation [12], seismic attenuation estimation [13] and many others.

However, there are several drawbacks occurred in practical applications of WVD. The main problem of application of WVD to multicomponent signal is an existence of cross-term interferences which may mask low-energy components, especially in the case of large dispersion of energy level of individual components [14]. In order to remove unwanted cross-term interferences, and improve TF resolution and separation ability of particular signal components several distributions have been developed, such as Cohen's class distributions. Such improvements were focused on design of appropriate kernel functions which allow matching their properties to a specific non-stationary signal processing task.

The enhancement of resolution and minimizing the cross-term interferences was reported in many practical studies, when the TFDs of the mentioned class was used instead of WVD. The improved TFDs have found many applications, including noise reduction [15], diagnosis of rotor machinery [9,14,16-18] and combustion engines [19], inspection of electrical power systems [20], characterization of complex physical processes [21], and many others. This is also proven by several comparative studies performed on synthetic multicomponent signals as well as on real signals acquired during machinery operation [3, 9, 22-28]. Nevertheless, the mentioned comparative studies are usually limited to the analysis of multicomponent, but still quite simple signals, and few TFDs.

The aim of this paper is a joint analysis of most of TFDs belonged to Cohen's class in terms of theoretical foundations as well as their application to identification of components in a multicomponent signal. For this purpose, the synthetic multicomponent signal with all types of components occurred in machinery during operation was generated and analyzed using various TFDs in order to characterize them in the view of admissibility in applications of signal processing in technical diagnostics problems. Further, selected TFDs were applied to the signals measured during operation of rolling bearings in order to verify the results of studies on synthetic signal as well as their effectiveness in identification of particular components in signals that represent their normal condition and a priori known faults. This leads to the alternative methodology of diagnosis of rolling bearing with respect to the common methods (see e.g. [29]).

2. THEORETICAL BACKGROUND

2.1. Cohen's class TFDs

The main idea of development of the TFDs that belong to the Cohen's class was an improvement of resolution of resulting TF distributions of signals as well as removing the unwanted cross-term interferences. All of these TFDs are resulted from smoothing of the WVD, where the only difference is an addition of a specific kernel function. Cohen, in his review paper [30], proposed a general form of a class of the discussed TFDs, which has the following form:

$$\mathrm{CCD}_x(t,f)=\int_{-\infty}^{+\infty}\int_{-\infty}^{+\infty}\phi(t-t',f-f')\mathrm{WVD}_x(t',f')\mathrm{d}t'\,\mathrm{d}f'=\int_{-\infty}^{+\infty}\int_{-\infty}^{+\infty}\Phi(\tau,\upsilon)A_x(\tau,\upsilon)\exp[j2\pi(t\upsilon-f\tau)]\mathrm{d}\tau\,\mathrm{d}\upsilon, \quad (4)$$

where

$$\phi(t,f)=\int_{-\infty}^{+\infty}\int_{-\infty}^{+\infty}\Phi(\tau,\upsilon)\exp[j2\pi(t\upsilon-f\tau)]\mathrm{d}\tau\,\mathrm{d}\upsilon, \quad (5)$$

$$A_x(\tau,\upsilon)=\frac{1}{2\pi}\int_{-\infty}^{+\infty}x\left(t+\frac{\tau}{2}\right)x^*\left(t-\frac{\tau}{2}\right)\cdot\exp(-j2\pi\upsilon t)\mathrm{d}t, \quad (6)$$

is the ambiguity function and $\Phi(\tau,\upsilon)$ is a kernel function in an ambiguity domain specific for particular types of distributions. From the great variety of available Cohen's TFDs 12 of them (including WVD presented above) were selected for further analyzes. The kernel functions for the basic Cohen's TFDs are as follows [6]:

- Spectrogram:
$$\Phi_{\mathrm{S}}(\tau,\upsilon)=A_x(\tau,\upsilon), \quad (7)$$
- Rihaczek:
$$\Phi_{\mathrm{RD}}(\tau,\upsilon)=\exp(j\pi\upsilon\tau), \quad (8)$$
- Page:
$$\Phi_{\mathrm{PD}}(\tau,\upsilon)=\exp(j\pi\upsilon|\tau|), \quad (9)$$
- Margenau-Hill:
$$\Phi_{\mathrm{MHD}}(\tau,\upsilon)=\cos(\pi\upsilon\tau), \quad (10)$$
- Born-Jordan:
$$\Phi_{\mathrm{BJD}}(\tau,\upsilon)=\mathrm{sinc}(\pi\upsilon\tau), \quad (11)$$
- Choi-Williams:
$$\Phi_{\mathrm{CWD}}(\tau,\upsilon)=\exp\left(-(2\pi\upsilon\tau/\sigma)^2\right), \quad (12)$$

where σ is a temporal scaling parameter,

- Zhao-Atlas-Marks:
$$\Phi_{\mathrm{ZAMD}}(\tau,\upsilon)=\exp\left(-(2\pi\upsilon\tau/\sigma)^2\right)\cos(2\pi\beta\tau), \quad (13)$$

where β is a spectral scaling parameter [31].

In order to improve TFDs presented above, several modifications of them have been developed. One type of such modifications is a type of pseudo-TRDs, e.g. pseudo Wigner-Ville distribution (PWVD), pseudo Page distribution (PPD) and pseudo Margenau-Hill distribution (PMHD). Such representations include a window function $h(\tau)$ which allows suppressing the interferences between signal components. The kernel functions for three latter cases are as follows [6]:

- PWVD:
$$\Phi_{\mathrm{PWVD}}(\tau,\upsilon)=h(\tau), \quad (14)$$
- PPD:
$$\Phi_{\mathrm{PPD}}(\tau,\upsilon)=h(\tau)\exp(j\pi\upsilon|\tau|), \quad (15)$$
- PMHD:
$$\Phi_{\mathrm{PMHD}}(\tau,\upsilon)=h(\tau)\cos(\pi\upsilon\tau). \quad (16)$$

For further enhancement of a resulting distribution, the smoothed PWVD (SPWVD) was introduced [32]. The difference lies in introducing an additional window function $g(t)$ which allows smoothing in time and frequency domains independently. Following this, the kernel function for this case takes a form [6]:

$$\Phi_{\mathrm{SPWVD}}(\tau,\upsilon)=h(\tau)\hat{g}(\upsilon), \quad (17)$$

where $\hat{\cdot}$ denotes Fourier transform.

2.2. Reassigned TFDs

Besides the effectiveness of improvements of initial WVD by smoothing operations performed in different ways for CCDs, some of cross-term interferences may remain in a time-frequency (or time-scale) plane. In order to overcome this drawback the reassignment method was proposed in [33], which is based on moving the mean energy of $\mathrm{CCD}_x(t,f)$ or $\mathrm{ACD}_x(t,a)$ at their specific locations – (t,f) or (t,a) to the center of gravity of a distribution [3]. Following this, one can obtain the reassigned Cohen's class distribution:

$$\mathrm{RCCD}_x(t,f)=\int_{-\infty}^{+\infty}\int_{-\infty}^{+\infty}\mathrm{CCD}_x(t,f)\delta\left(t'-\hat{t}(t,f)\right)\cdot\delta\left(f'-\hat{f}(t,f)\right)\mathrm{d}t\,\mathrm{d}f, \quad (18)$$

where

$$\hat{t}(t,f)=t-\frac{\int_{-\infty}^{+\infty}\int_{-\infty}^{+\infty}\tau\phi(\tau,\upsilon)\mathrm{WVD}_x(t-\tau,f-\upsilon)\mathrm{d}\tau\,\mathrm{d}\upsilon}{\int_{-\infty}^{+\infty}\int_{-\infty}^{+\infty}\phi(\tau,\upsilon)\mathrm{WVD}_x(t-\tau,f-\upsilon)\mathrm{d}\tau\,\mathrm{d}\upsilon}, \quad (19)$$

$$\hat{f}(t,f)=f-\frac{\int_{-\infty}^{+\infty}\int_{-\infty}^{+\infty}\upsilon\phi(\tau,\upsilon)\mathrm{WVD}_x(t-\tau,f-\upsilon)\mathrm{d}\tau\,\mathrm{d}\upsilon}{\int_{-\infty}^{+\infty}\int_{-\infty}^{+\infty}\phi(\tau,\upsilon)\mathrm{WVD}_x(t-\tau,f-\upsilon)\mathrm{d}\tau\,\mathrm{d}\upsilon}. \quad (20)$$

Following this reassignment method various Cohen's class distributions with enhanced parameters can be obtained. For further studies the following 4 reassigned distributions were selected: reassigned PMHD, PWVD, SPWVD and reassigned spectrogram, whose forms can be obtained from (18).

3. ANALYSIS OF SYNTHETIC MULTICOMPONENT SIGNAL

3.1. Description of the synthetic signal

The synthetic signal was modeled in the Matlab® environment and contains the following components. Firstly, three harmonics with frequencies of 100 Hz, 140 Hz, and 180 Hz, respectively were composed together. Next, fourth harmonic with a frequency of 300 Hz and duration of 4 s was added to the rest. In the fourth second two chirp signals, linear (with a starting frequency of 300 Hz and ending frequency of 100 Hz) and quadratic (with a starting frequency of 300 Hz and ending

frequency of 500 Hz), respectively, were simulated with a duration of 6 s. Additionally, two pulse signals with magnitudes of 10 and 5, and appearance at fifth and eighth second, respectively, were added to the signal. Finally, noise with a magnitude of 0.1 was added to the rest of components. The particular components of the signal are described by the following equations:

$$x_{1,\ldots,3}(t) = A_1 \sin\left(2\pi f_{1,\ldots,3} t\right), \tag{18a}$$

$$x_4(t_1) = A_1 \sin\left(2\pi f_4 t_1\right), \tag{18b}$$

$$x_5(t_2) = A_1 \sin\left(2\pi f_5(t_2) t_2\right),\ f_5(t_2) = f_5 + kt_2, \tag{18c}$$

$$x_6(t_2) = A_1 \sin\left(2\pi f_6(t_2) t_2\right),\ f_6(t_2) = f_6 + kt_2^2, \tag{18d}$$

$$x_7(t) = A_2 \prod(t_3),\ x_8(t) = A_3 \prod(t_4), \tag{18e}$$

$$x_9(t) = A_4\, \mathrm{rand}(t), \tag{18f}$$

and are added up. A total duration of the signal is 10 s with a step of 0.001 s. In order to visualize the modeled multicomponent signal the spectrogram was chosen (see Fig.1). Moreover, the spectrogram was selected as a reference of time-frequency representation with respect to the considered TFDs.

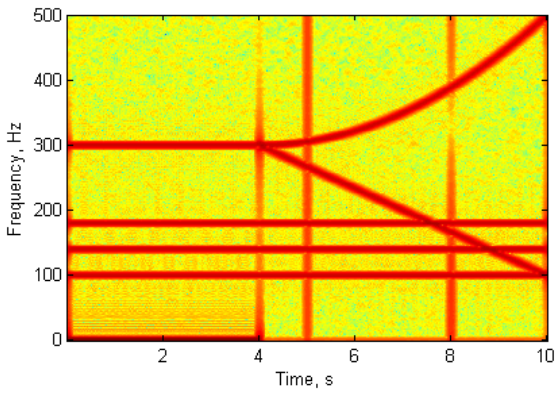

Fig.1. Spectrogram of the modeled multicomponent signal

In the presented spectrogram, one can observe that sudden change of fifth and sixth components from zero- to non-zero-value at fourth second causes an appearance of additional peak which is quite similar to the pulse signals at fifth and eighth second. All components are clearly visible in this spectrogram.

3.2. Component identification in a synthetic signal – a comparative study

In order to observe the performance of various TFDs described in section 2, the comparative study was performed. For this purpose the Time-Frequency Toolbox for use with Matlab® [34] was used. The modeled multicomponent signal was subjected to transformation into time-frequency domain using above-described TFDs. The resulting time-frequency representations are shown in Figs. 2-16.

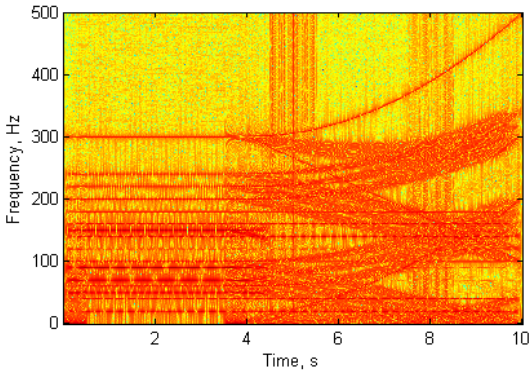

Fig.2. Time-frequency representation of the synthetic signal using WVD

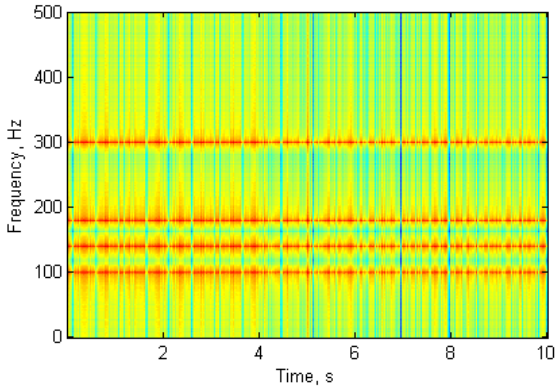

Fig.3. Time-frequency representation of the synthetic signal using RD

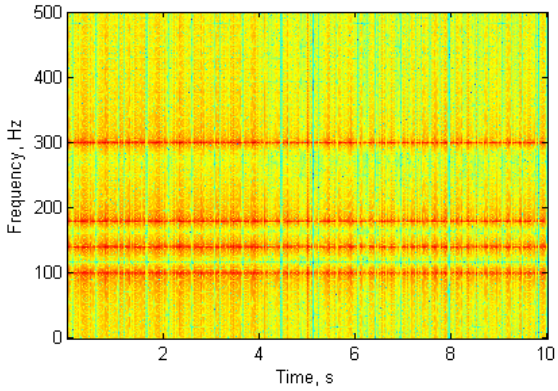

Fig.4. Time-frequency representation of the synthetic signal using PD

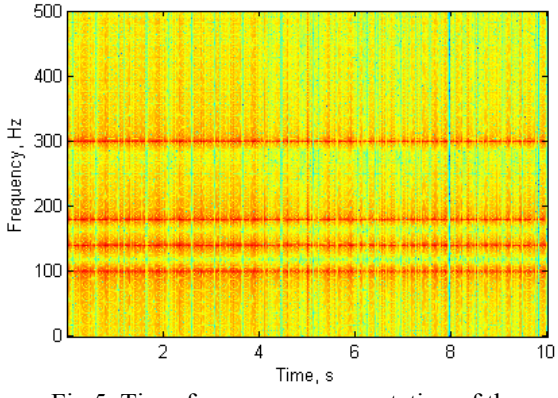

Fig.5. Time-frequency representation of the synthetic signal using MHD

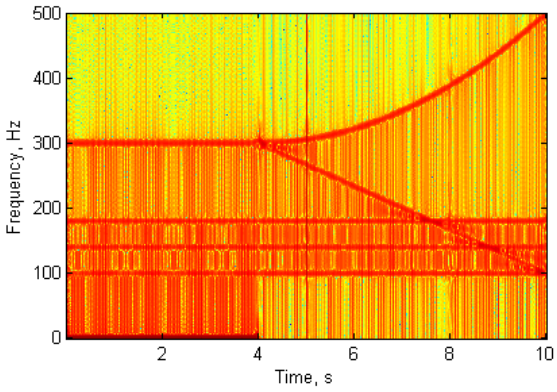

Fig.6. Time-frequency representation of the synthetic signal using BJD

From the presented representations one can observe that there is a group of TFDs which detects harmonic and pulse components (only in the case of RD) well, but remains insensitive to non-stationary components in the analyzed signal. This can be observed for Rihaczek, Page and Margenau-Hill distributions (Figs.3-5).

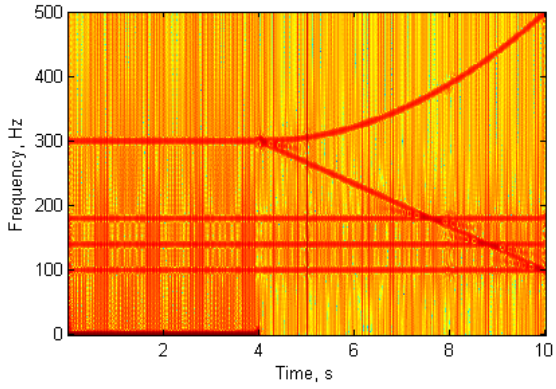

Fig.7. Time-frequency representation of the synthetic signal using CWD

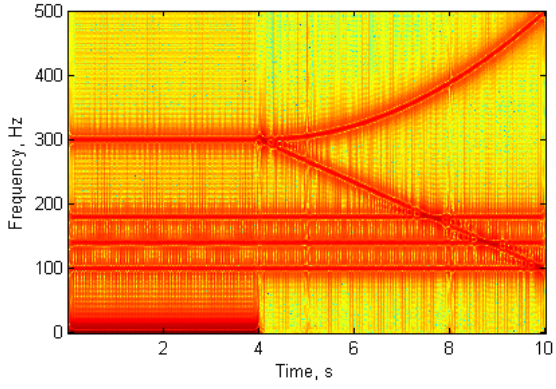

Fig.8. Time-frequency representation of the synthetic signal using ZAMD

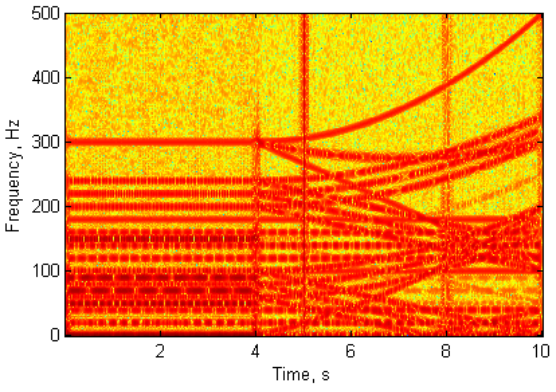

Fig.9. Time-frequency representation of the synthetic signal using PWVD

Another group of TFDs from the considered ones, namely Wigner-Ville (Fig.2), pseudo-Wigner-Ville (Fig.9), and reassigned pseudo-Wigner-Ville (Fig.15) distributions, detects all types of components well, but produces artefacts in the time-frequency representations (caused by interference of two auto-terms in (3)) which makes the proper interpretation of the resulting spectrum difficult.

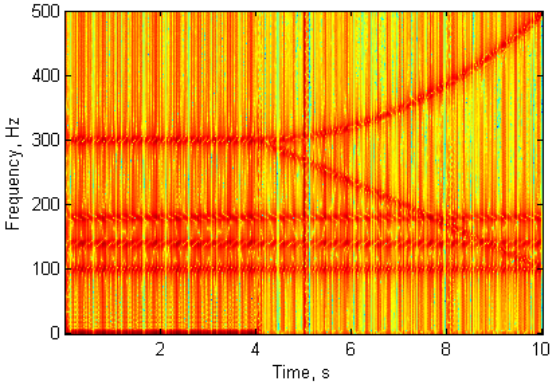

Fig.10. Time-frequency representation of the synthetic signal using PPD

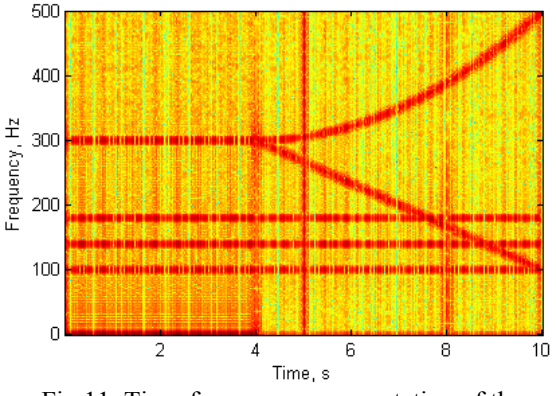

Fig.11. Time-frequency representation of the synthetic signal using PMHD

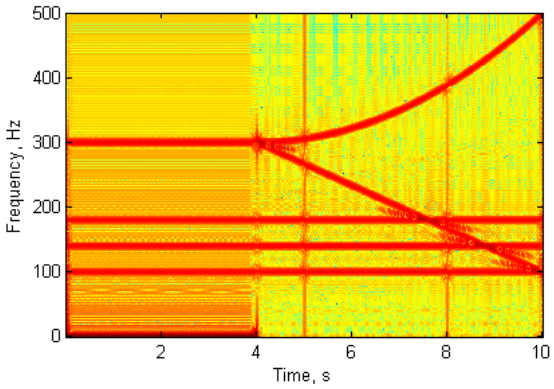

Fig.12. Time-frequency representation of the synthetic signal using SPWVD

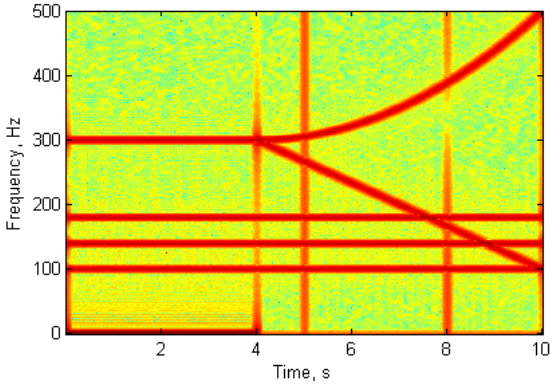

Fig.13. Time-frequency representation of the synthetic signal using reassigned spectrogram

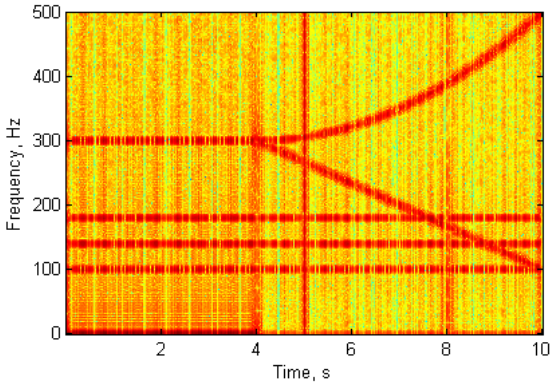

Fig.14. Time-frequency representation of the synthetic signal using reassigned PMHD

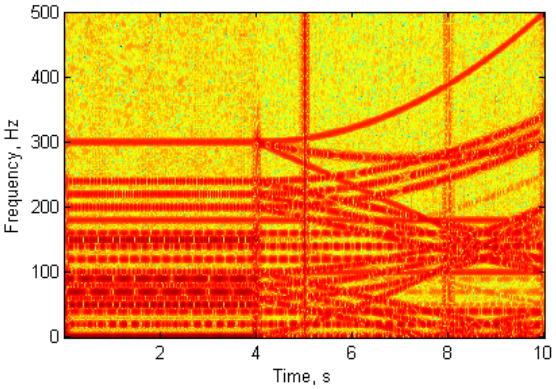

Fig.15. Time-frequency representation of the synthetic signal using reassigned PWVD

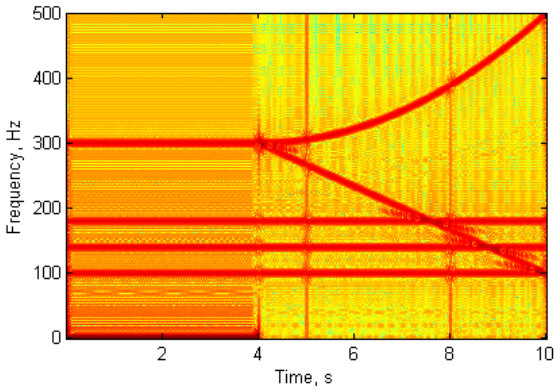

Fig.16. Time-frequency representation of the synthetic signal using reassigned SPWVD

This induces another problem with WVD-type spectra – the appearance of negative values that has no physical justification which is their serious drawback.

Observing BJD, CWF and ZAMD spectra (Figs. 6-8), which have similar formulations – see (11)-(13), one can conclude that both harmonic and non-stationary components of the analyzed signal are well localized in time and frequency, however the blurring of the identified components discredits these distributions from further consideration. Moreover, the pulse components are almost undetectable in the considered spectra.

The pseudo versions of particular distributions contain a window function in their definitions that allows reducing interference terms and causes that the resulting spectra are smoother in frequency. This improves significantly the detectability of components in spectra (cf. Fig.4 and Fig.10, Fig.5 and Fig.11).

The smoothed version of the pseudo-WVD contains two independent windows in order to perform smoothing both in time and frequency domains which, as a result, gives precise localization of harmonics, non-linear and transient components of the signal (see Fig.12). Note that in this case very good localization of the pulse components is observed, and in the same time the peak in fourth second is almost undetectable. One can also notice that the reassigned version of SPWVD (Fig.16) does not contribute to any improvements with respect to SPWVD.

The reassignment allows for obtaining TFD spectra with better concentration of energy both in time and frequency domains, which improves their readability. In the following study the effects of reassignment is not clearly visible, however, considering theoretical fundamentals of the reassignment procedure [6] it is suitable to consider the reassigned versions of TFDs.

Based on the performed comparative study one can select the following TFDs which detected well all components of the synthetic signal typical in vibroacoustic diagnostics of machinery: reassigned spectrogram, reassigned PMHD, and reassigned SPWVD. These TFDs were applied for signal

components detection in rolling bearings, described in the next section.

4. IDENTIFICATION OF COMPONENTS OF ROLLING BEARINGS VIBRATION SIGNALS

The signals of radial acceleration were acquired on the laboratory test rig with a rolling bearing from the top of the tested bearing casing (SKF® type SNL) using the PCB® Piezotronics T352C34 piezoelectric accelerometer. The tested bearing considered in this study contained 9 rolling elements and a fault of rolling element. The duration of each measurement was 4.8 s with a sampling frequency of 51.2 kHz. The rotational speed of the test rig equaled 1603 rpm. Further details on acquisition, resonant frequencies and properties of a signal can be found in [35]. The time-domain representation of the analyzed signal is presented in Fig.17.

In order to identify typical signal components of the tested bearing, in particular the components responsible for occurrence of the damage of rolling element, the time-frequency spectra were determined using TFDs selected in the previous section. The resulting spectra are presented in Fig.18. The frequency range was limited to 1250 Hz.

The presented spectra show the occurrence of three harmonic components (with central frequencies of 450 Hz, 650 Hz and 1095 Hz) and pulse components which repeat periodically and result from the damage of the rolling elements. These periodic impacts excite natural frequencies of

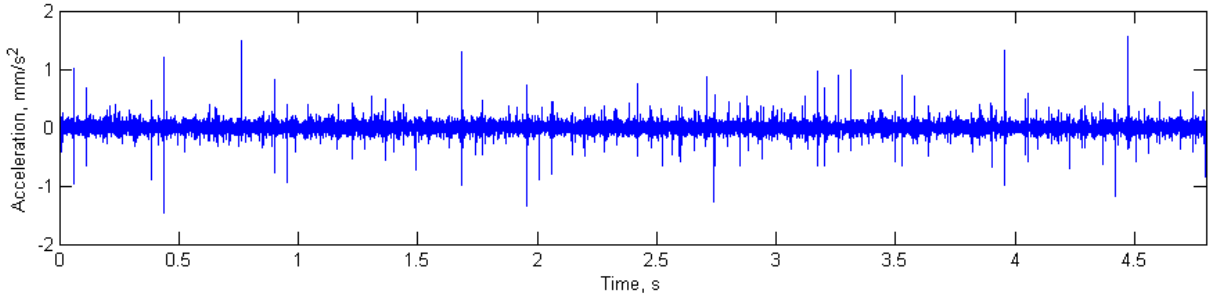

Fig.17. Time-domain representation of the analyzed signal or the rolling bearing with the fault

the bearing elements. They also may excite sidebands around the resonance frequencies (which is one of the reasons of blurring the harmonics on the spectra presented in Fig.18) as well as occurrence of components which are the multiplications of bearing defect frequencies.

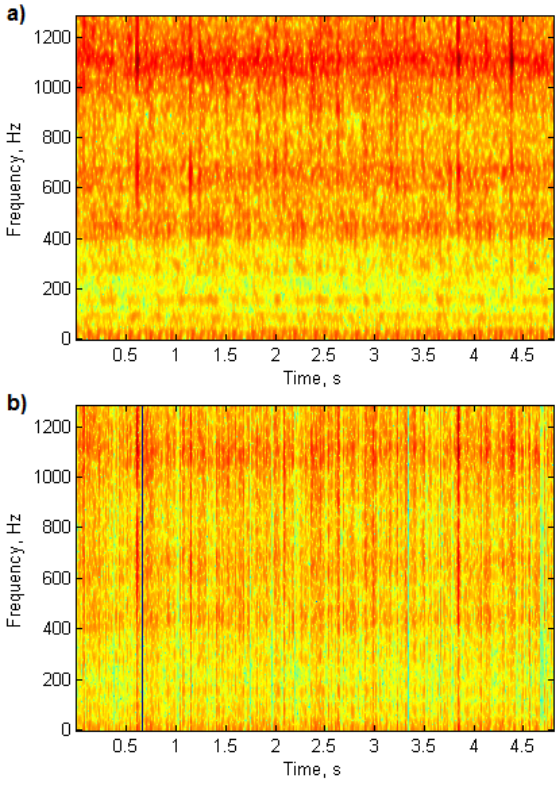

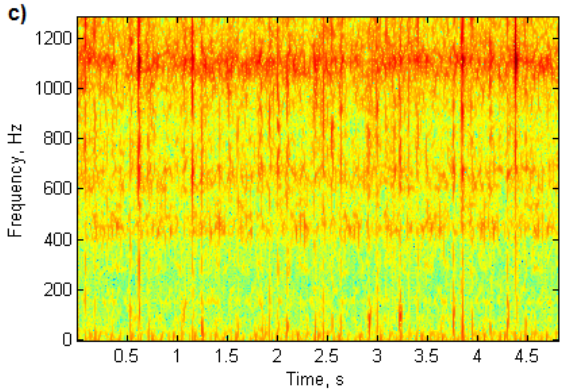

Fig.18. Spectrum of vibration signal of bearing obtained using a) reassigned spectrogram, b) reassigned PMHD, c) reassigned SPWVD

One can also observe in Fig.18 that the considered TFDs selected in the previous sections are suitable for detection of all above-mentioned components, however, the detectability of these components differs. The spectrum obtained using reassigned spectrogram distribution allows for detection of three harmonics and pulses, however all of these components are blurred which may cause difficulties in localization both in time and frequency domains. The reassigned PMHD makes possible detection of pulse components with the highest magnitudes only, while the rest of pulse components as well as harmonic components are weakly detectable. The best results were obtained from the reassigned SPWVD which provides good sharpness of both types of components, and thus,

provides good localization in time and frequency domains. Considering this, in the case of diagnosing rolling bearings the reassigned SPWVD seems to be the most accurate distribution from the previously analyzed ones, however, at the expense of computational complexity.

5. CONCLUSIONS

The performed studies allow comparing various types of TFDs and their applicability in vibroacoustic diagnostics problems. Based on comparative study performed on synthetic multicomponent signal with stationary and non-stationary components it was possible to analyze a performance of 16 TFDs belonged to Cohen's class, and their smoothed and reassigned versions. Based on these results it was possible to select the most suitable TFDs that allow detecting all types of desired components. The selected TFDs was applied to obtain spectra of vibration signal of rolling bearing with faulty rolling element. The final analysis shows the best effectiveness of the reassigned SPWVD which can be applied in similar analyses.

REFERENCES

1. Muszynska A. Vibrational diagnostics of rotating machinery malfunctions. International Journal of Rotating Machinery, 1995; 1:237-266. http://dx.doi.org/10.1155/S1023621X95000108
2. Sabnavis G., Kirk R.G., Kasarda M., Quinn D. Cracked shaft detection and diagnostics: A literature review. Shock and Vibration Digest, 2004; 36:287-296. http://dx.doi.org/10.1177/0583102404045439
3. Feng Z., Liang M., Chu F. Recent advances in time-frequency analysis methods for machinery fault diagnosis: A review with application examples. Mechanical Systems and Signal Processing, 2013; 38:165-205. http://dx.doi.org/10.1016/j.ymssp.2013.01.017
4. Bachmann G., Narici L., Beckenstein E. Fourier and Wavelet Analysis. New York: Springer, 2000.
5. Mallat S.G. A Wavelet Tour of Signal Processing: The Sparse Way. San Diego, CA: Academic Press, 2009.
6. Hlawatsch F., Auger F., Eds., Time-Frequency Analysis. Concepts and Methods. London: ISTE, 2008.
7. Andria G., Savino M., Trotta A. Application of Wigner-Ville distribution to measurements on transient signals. IEEE Transactions on Instrumentation and Measurement, 1994; 43:187-193. http://dx.doi.org/10.1109/19.293418
8. Staszewski W.J., Worden K., Tomlinson G.R. Time-frequency analysis in gearbox fault detection using the Wigner-Ville distribution and pattern recognition. Mechanical Systems and Signal Processing, 1997; 11:673-692. http://dx.doi.org/10.1006/mssp.1997.0102
9. Bartelmus W., Zimroz R. Vibration condition monitoring of planetary gearbox under varying external load. Mechanical Systems and Signal Processing, 2009; 23:246-257. http://dx.doi.org/10.1016/j.ymssp.2008.03.016
10. Climente-Alarcon V., Antonino-Daviu J.A., Riera-Guasp M., Puche-Panadero R., Escobar L. Application of the Wigner-Ville distribution for the detection of rotor asymmetries and eccentricity through high-order harmonics. Electric Power Systems Research, 2012; 91:28-36. http://dx.doi.org/10.1016/j.epsr.2012.05.001
11. Kim Y.B., Kim S.J., Chung H.D., Park Y.W., Park J.H. A study on technique to estimate impact location of loose part using Wigner-Ville distribution. Progress in Nuclear Energy, 2003; 43:261-266. http://dx.doi.org/10.1016/S0149-1970(03)00033-7
12. Zhu Y.M., Goutte R., Amiel M. On the use of two-dimensional Wigner-Ville distribution for texture segmentation. Signal Processing, 1993; 30:329-353. http://dx.doi.org/10.1016/0165-1684(93)90016-4
13. Yandong L., Xiaodong Z. Wigner-Ville distribution and its application in seismic attenuation estimation. Applied Geophysics, 2007; 4:245-254. http://dx.doi.org/10.1007/s11770-007-0034-7
14. Urbanek J., Barszcz T., Zimroz R., Antoni J. Application of averaged instantaneous power spectrum for diagnostics of machinery operating under non-stationary operational conditions. *Measurement*, 2012, 45:1782-1791. http://dx.doi.org/10.1016/j.measurement.2012.04.006
15. Hassanpour H. A time-frequency approach for noise reduction. Digital Signal Processing, 2008; 18:728-738. http://dx.doi.org/10.1016/j.dsp.2007.09.014
16. Baydar N., Ball A. A comparative study of acoustic and vibration signals in detection of gear failures using Wigner-Ville distribution. Mechanical Systems and Signal Processing, 2001, 15:1091-1107. http://dx.doi.org/10.1006/mssp.2000.1338
17. Ma J., Wu J., Yuan X. The fault diagnosis of the rolling bearing based on the LMD and time-frequency analysis. International Journal of Control and Automation, 2013; 6:357-376.
18. Antoniadou I., Dervilis N., Papatheou E., Maguire A.E., Worden K. Aspects of structural health and condition monitoring of offshore wind turbines. Philosophical Transactions of the Royal Society A, 2015; 373:20140075. http://dx.doi.org/10.1098/rsta.2014.0075
19. Stanković L.J., Böhme J.F. Time-frequency analysis of multiple resonances in combustion engine signals. Signal Processing, 1999; 79:15-28. http://dx.doi.org/10.1016/S0165-1684(99)00077-8
20. Cheng J.Y., Hsieh C.T., Huang S.J., Huang C.M. Application of modified Wigner distribution method to voltage flicker-generated signal studies. International Journal of Electric Power and Energy Systems, 2013; 44:275–281. http://dx.doi.org/10.1016/j.ijepes.2012.07.045
21. Xu L.Q., Hu L.Q., Chen K.Y., Li E.Z. Time-frequency analysis of nonstationary complex magneto-hydro-dynamics in fusion plasma signals using the Choi-Williams distribution. Fusion Engineering and Design, 2013; 88:2767-2772. http://dx.doi.org/10.1016/j.fusengdes.2013.04.017
22. Jones D.L., Parks T.W. A resolution comparison of several time-frequency representations. IEEE Transactions on Signal Processing, 1992; 40:413-420.

http://dx.doi.org/10.1109/ICASSP.1989.266906
23. Hlawatsch F., Manickam T.G., Urbanke R.L., Jones W. Smoothed pseudo-Wigner distribution, Choi-Williams distribution, and cone-kernel representation: Ambiguity-domain analysis and experimental comparison. Signal Processing, 1995; 43:149-168. http://dx.doi.org/10.1016/0165-1684(94)00150-X
24. Hammond J.K., White P.R. The analysis of nonstationary signals using time-frequency methods. Journal of Sound and Vibration, 1996; 190:419-447. http://dx.doi.org/10.1006/jsvi.1996.0072
25. Ma N., Vray D., Delachartre P., Gimenez G. Time-frequency representation of multicomponent chirp signals. Signal Processing, 1997; 56:149-155. http://dx.doi.org/10.1016/S0165-1684(96)00163-6
26. Wang Y., Jiang Y. Generalized time-frequency distributions for multicomponent polynomial phase signals. Signal Processing, 2008; 88:984-1001. http://dx.doi.org/10.1016/j.sigpro.2007.10.016
27. Sejdić E., Djurović I., Jiang J. Time-frequency feature representation using energy concentration: An overview of recent advances. Digital Signal Processing, 2009; 19:153-183. http://dx.doi.org/10.1016/j.dsp.2007.12.004
28. Hansson-Sandsten M. Multitaper Wigner and Choi-Williams distributions with predetermined Doppler-lag bandwidth and sidelobe suppression. Signal Processing, 2011; 91:1457-1465. http://dx.doi.org/10.1016/j.sigpro.2010.10.010
29. Randall R.B., Antoni J. Rolling element bearing diagnostics – A tutorial. Mechanical Systems and Signal Processing, 2011; 25:485-520. http://dx.doi.org/10.1016/j.ymssp.2010.07.017
30. Cohen L. Time-frequency distributions – A review. Proceedings of IEEE, 1989; 77:941-981. http://dx.doi.org/10.1109/5.30749
31. Papanderou A., Faye Boudreaux-Bartels G. Distributions for time-frequency analysis: a generalization of Choi-Williams and Butterworth distribution. Proceedings of IEEE International Conference on Acoustics, Speech and Signal Processing, San Francisco, CA, 1992; 5:181-184. http://dx.doi.org/10.1109/ICASSP.1992.226628
32. Flandrin P., Martin W. A general class of estimators for the Wigner-Ville spectrum of nonstationary processes. Bensoussan A., Lions J.L., Eds., Systems Analysis and Optimization of Systems, Lecture Notes in Control and Information Sciences, 1984; 62:15-23. http://dx.doi.org/10.1007/BFb0004941
33. Auger F., Flandrin P. Improving the readability of time-frequency and time-scale representations by the reassignment method. IEEE Transactions on Signal Processing, 1995; 43:1068-1089. http://dx.doi.org/10.1109/78.382394
34. Auger F., Flandrin P., Gonçalvès P., Lemoine O. Time-Frequency Toolbox. CNRS France, Rice University, 1996, http://tftb.nongnu.org.
35. Katunin A., Wysogląd B., Gawron V. Condition monitoring of roller bearings based on estimation of Hurst exponents of vibration signals. Scientific Problems of Machines Operation and Maintenance, 2012; 47: 51-62.

Received 2016-04-14
Accepted 2016-05-31
Available online 2016-06-04

Andrzej KATUNIN, Ph.D., D.Sc., is an assistant professor at the Institute of Fundamentals of Machinery Design of Silesian University of Technology in Gliwice, Poland. His areas of research cover mechanics and non-destructive testing of composites, advanced signal and image processing, technical diagnostics, wavelets and fractals theory and applications. He is a member of the Polish Society of Technical Diagnostics since 2015.